Energy saving magnets for beam lines

Journal of Physics: Conference Series **2687** (2024) 082049 doi:10.1088/1742-6596/2687/8/082049

Energy saving magnets for beam lines

L. Rossi[1,2], **S. Mariotto**[1,2], **S. Sorti**[1,2]

[1]Università degli Studi di Milano, Dipartimento di Fisica, Milano, Italy, IT
[2]INFN Sezione di Milano, Laboratorio di Acceleratori e Superconduttività Applicata, Segrate, Italy, IT

E-mail: lucio.rossi@unimi.it

Abstract. Beam lines magnets for high rigidity particles can have a large power dissipation. In presence of a high duty cycle, this translates in a considerable amount of energy waste. The call for sustainability of large research infrastructures, like particle accelerator centers, and the recent increase of the cost of energy, require to take measures to reduce the energy consumption, even at cost of moderate investment. A study program called ESABLIM (Energy SAving Beam LIne Magnets) has been set up at the LASA lab of University and INFN Milano, aimed at revamping existing normal-conducting magnets for beam lines with the target of cutting the peak power by a factor 10 to 20 and reducing the energy consumption by factor 5 or more. The idea is to replace the water cooled coils of iron-dominated magnets with new superconducting coils cooled at 10-20 K by means of a cryocooler, while to reusing the iron yoke pole assembly. We envisage using MgB_2 for its moderate cost, however, high temperature superconductors (HTS) will also be considered as conductor. We present the first advanced design for revamping of a large bending dipole in a hadron therapy center, and the conceptual design for magnets in a nuclear physics laboratory and we try to define the domain where this transformation of normal-conducting into super-ferric magnets can be technically and economically advantageous.

1. Introduction

Recent studies for heavy ion therapy center development,[1], outlined that resistive magnets play an important role in the total energy consumption of such large research facilities dealing with relatively high rigidity particles. However, the same consideration can be applied to fundamental physics research centers dealing with hadron beams. The recent rise in energy price and the unavoidable demand for sustainability of research infrastructure have made superconducting coils in iron dominated magnets, called superferric layout, an attractive alternative to save energy. Two approaches can be used for superferric designs: 1) replacement of the resistive coil with a superconducting configuration and reusing the existing iron yoke, and 2) complete redesign of the magnet to fully exploit the potential of superconductors, which may result in a higher total magnet cost. If the gap between the superconducting coil and iron yoke is too large for the mechanical frame and cryogenic system, the second approach may be necessary. In this paper, two magnet designs (shown in Fig. 1) are discussed as the first case study to evaluate the feasibility of the project. The designs aim to replace the copper coils with a higher current density superconducting configuration while using the same iron yoke around the magnet. The first design is based on the Centro Nazionale di Adroterapia Oncologica (CNAO, Pavia, IT) 90° bending dipole magnet currently installed in the vertical beam line of the proton (60-250 MeV) and heavy carbon ions (120-400 MeV/u) synchrotron. The 70 tons resistive magnet, designed in 2006 by SIGMAPHI, provides 1.74 T with a field quality of ±2 units (10^{-4}) in a bore area

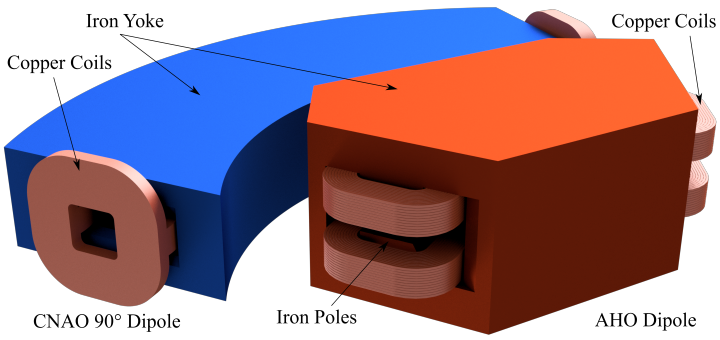

Figure 1. Rendering of the resistive magnet designs of the CNAO 90° dipole and PSI AHO dipole configurations

of 200x200 mm^2 and has a bending radius of 3.65 m. The two magnet ends are tilted with 21° (entrance) and 30° (exit) to provide edge focusing effects on the particles. The second design is based on the AHO magnet currently installed in the underground beam line towards the SINQ neutron spallation source at the Paul Scherrer Institute (PSI), Zurich, CH. Initially used as a switching magnet, the 50 tons resistive bending dipole provides 1.45 T on a 2.78 m bending radius for a 64° angle. The CNAO dipole is designed to be ramped to the nominal current of 2.28 kA in 10 s (700 kW of peak electrical power) performing a stair step energization according to the required medical treatment while the AHO magnet runs continuously from mid-May to mid-December taking up to 190 kW. Considering the duty-cycle of the two magnets, the first magnet is expected to consume 282.2 MWh/year while the PSI dipole consumes 715 MWh/year.

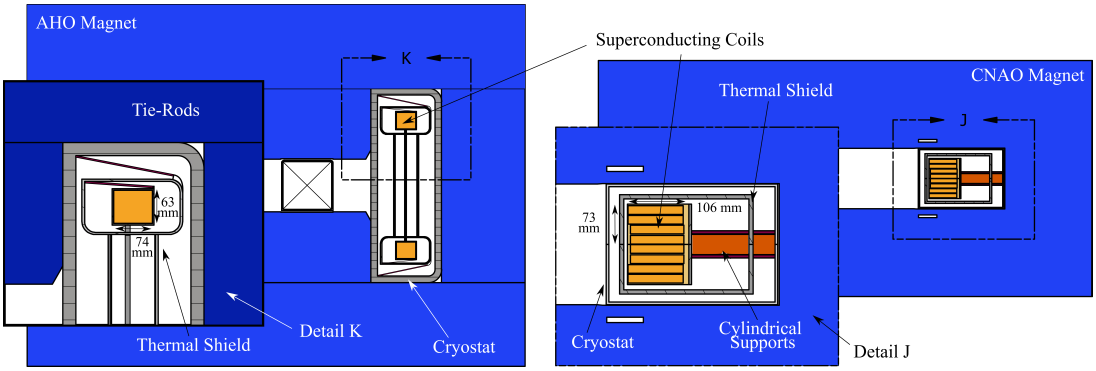

Figure 2. Cross-section of the superconducting design for the AHO magnet and CNAO 90° dipole. A zoomed view of the magnet assembly details is reported. The mechanical structure, the thermal shield and cryostat cross-section are visible.

2. Superconducting EM Design

To obtain a high magnet stability, the superconducting configuration is designed to work at a margin of 40% at least on the magnet load-line. The total coil current is equal to the resistive configuration, see Table 1, and the conductor design has been optimized to obtain high thermal stability and minimize the AC losses during ramping. Since the INFN LASA team already has experience with the winding of MgB_2 conductor, [2, 3, 4, 5], a first proposal using magnesium diboride is here presented. Evaluation of HTS (REBCO) conductor as alternative is a next

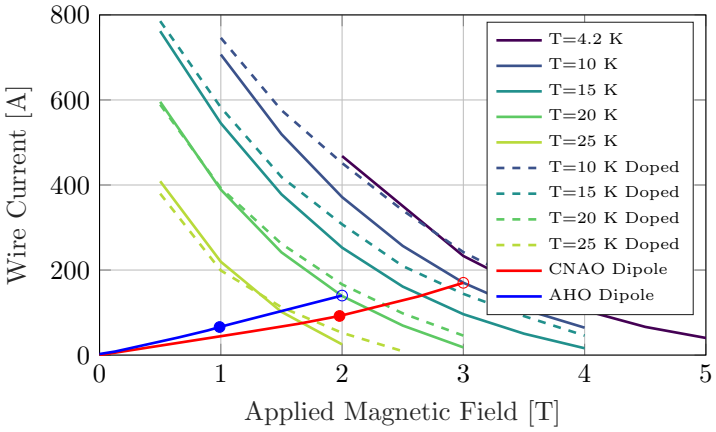

Figure 3. Load-line of the two superconducting magnet designs considered in the study feasibility evaluation

step of the project. In order to deal with the strain-sensitive behaviour of the MgB_2 conductor, currently limited to a minimum bending radius of 100 mm for a 1 mm wire ([6]) a rope conductor design has been considered, like already developed in [7], with a 3 to 4 ratio (3 superconducting wires and 4 copper wires) for the CNAO magnet coil design and a 4 to 3 ratio for the AHO magnet coil design. The rope is insulated with a 0.07 mm fiberglass braid used widely in superconducting magnets developed for the HL-LHC project and the coil ground insulation relies on BT resin S2 glass-fiber reinforced material ([8],[9]). The CNAO magnet features an asymmetric superconducting coil design, optimized to work at T=10 K and peak magnetic field B_{peak}=1.98 T. The geometry is shaped to satisfy the magnetic field quality requirement on the 200x200 mm^2 area and compensate the magnet geometric bending effect. A rectangular coil cross-section (74x63 mm^2) has been considered for the AHO magnet coil design working at T=20 K and B_{peak} = 0.99 T with a margin on the load-line equals to 50% and a temperature margin of 8 K. Because of the iron pole profile, the superconductor experiences mostly the self-field far from the iron yoke: thus, the superconductor magnetization generates no appreciable field contribution in the aperture as obtained in the CNAO 90° dipole cross-section.

3. Thermo-Mechanical structure

The mechanical assembly of the two magnet designs has been optimized to withstand the electromagnetic force density at nominal current while minimizing heat conduction during normal operation. For the CNAO 90° Dipole, a reinforcement bar was designed to prevent conductor deformations due to peak stresses caused by a calculated force linear density of 0.14

Table 1. Main parameters of the resistive and superconducting coil designs for the AHO and CNAO magnets

	AHO		CNAO	
	Resistive	Super.	Resistive	Super.
I_{op}	1 kA	300 A	2.28 kA	276 A
Cable	18.5 mm	⌀ 3 mm	39.8 mm	⌀ 3 mm
Turns	12x12	22x22	8x10	20x31/32
Coil	250x245 mm^2	74x63 mm^2	398x114 mm^2	106x73 mm^2

MN/m on one single coil. Two solutions for mechanical coil support are under evaluation: G10 tie rods or G10 reinforced cylindrical supports connecting the coil support to the thermal shield and the thermal shield to the cryostat. In Fig. 2 the cylindrical support design is represented. Two different cylinder lengths (coil support to thermal shield and thermal shield to cryostat) are optimized to minimize heat load on the superconductor and maintain the thermal shield at a minimum operating temperature of 60 K. The thermal shield thickness is increased to enhance power extraction and covered with a 30 multi-layers MLI sheet to minimize radiation heat load. The same approach has been used for the AHO design. The planar coils are surrounded by a 3 mm thick stainless-steel collar supported by a distributed set of tie-rods (⌀=4mm) connected to the thermal shield. In addition, the aluminum thermal shield, covered again by 30 layers of MLI, is supported with similar tie rods (⌀=6mm) connecting to the cryostat. The mechanical structure for both magnets limits coil deformation to a 1 mm displacement and reduces mechanical strain on single conductors to below the 0.2% threshold at which the superconductor critical current starts to degrade [10].

4. Thermal Design

The calculation of AC losses and power loads is vital to evaluate the coil operating temperature and magnet stability. The power losses during the steady-state AHO magnet powering are not reported here and considered negligible in the magnet cycle. Instead, for the CNAO 90° dipole, the superconductor AC losses have been calculated using a standard equivalent magnetization model considering the superconductor hysteresis, the inter-filament (IFCC) and inter-strand (ISCC) coupling currents [11, 12, 13]. The superconductor hysteresis losses depend on the wire critical current density reported in Fig. 3. For the IFCC calculation, the same approach used in [14, 15] has been adopted modeling the MgB_2 wire cross-section. The transversal induced electric field potential can be described as in equation 1 depending on the magnetic field variation rate $\dot{B}_s$, the twist pitch of the filaments inside the wire $L_{p,f}$ and the wire diameter d_s^*.

$$V(\varphi) = -2d_s^* \left(\frac{L_{p,f}}{2\pi}\right) \dot{B}_s \cos(\varphi) \; or \; V(x) = \frac{\dot{B}_s}{2\pi} L_{p,f} x \tag{1}$$

A static electric simulation (Fig. 4, left) is used to assess induced eddy currents in the wire and determine the transversal effective resistivity, necessary for calculating the intrinsic decay time of the IFCC. The ISCC calculation follows a similar approach, treating the rope as a large single strand with real strands acting as filaments. The simulation assumes no contact resistance between strands, with a twist pitch length of 150 mm (Fig. 4). The power losses calculated with the model are then fitted as function of the external magnetic field ramp rate to be used in the superconducting coil power losses calculation and maximum operating temperature in the coils, see Table 2.

The material properties of the coil, like transversal/longitudinal thermal conductivity and enthalpy are calculated averaging over the materials fraction inside the coil volume. Two Cryomech cryocoolers (Al63 and Al60), [16], are used to independently cool the superconducting coils and thermal shield of the AHO magnet. This results in a maximum operating temperature of 20.8 K on one side of the magnet, while maintaining a maximum temperature increment of ¡10 K on the thermal shield surface opposite to the cryocooler side. For the CNAO magnet, a simplified straight thermal model involving 1/4 of a superconducting coil has been used to evaluate the maximum operating temperature considering to cool down the entire coil and thermal shield from both sides of the magnet. The peak operating temperature in the steady state simulation (slightly conservative compared to the time dependent simulation in the magnet powering cycles, see [17]) is equal to 12.7 K resulting in a temperature margin of 10.1 K. The superconducting coil and the thermal shield are cooled down with 4 Cryomech two stage pulsed

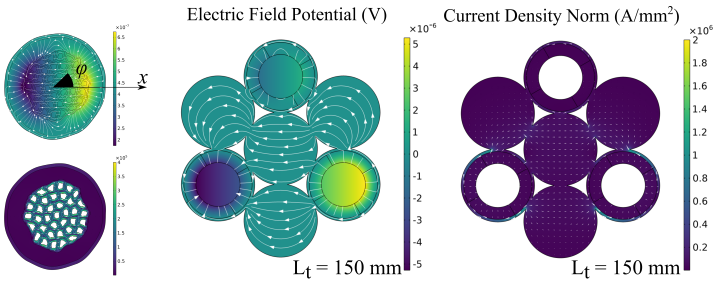

Figure 4. EM simulations of induced coupling currents in the MgB_2 wire and rope cross-sections used in the CNAO 90° dipole superconducting coil.

tube cryocoolers PT425 while two additional cryocooler are dedicated for the current leads. The AHO superconducting design (18.8 MWh/year) exhibits an energy scaling factor of 40 when compared to the average yearly energy consumption of the resistive configurations (715 MWh/year). In contrast, the CNAO superconducting design (68.8 MWh/year vs resistive design @ 282.2 MWh/year) achieves a reduction in energy consumption with a factor of 4 mainly due to the relatively low 10 K operating temperature. A solution operating at 20 K, under way, should increase the energy saving factor to 6/8 reducing the cryocoolers cost of energy extraction at room temperature.

5. Conclusions

The analysis reported here show the feasibility of MgB_2 superconducting coils for efficient beam line superferric cryogen-free magnets. The AHO magnet design feature a factor of up to 40 in yearly reduction averaged energy consumption, while ramped magnet configurations strongly depend on the selected operating temperature and the balance between power losses and heat extraction. A new design with superconducting coils cooled at 20 K is expected to significantly improve the performance of the CNAO magnet. Moving forward, complete 3D finite element models will be used to precisely address real operating temperatures during ramped magnet operating cycles considering the cryocooler time response. Further studies will deal with new resistive magnet designs, quench protection studies and will address the range of magnet parameters suitable for MgB_2 and REBCO superconducting coil configurations.

Table 2. Heat load for the AHO and CNAO dipoles and AC losses in each of the CNAO 90° Dipole coils: hysteretic, inter-filament and inter-strands coupling currents.

Magnet	Type	Q_{sup} [W]	Q_{CL} [W]	Q_{rad} [W]	Q_{tot} [W]
AHO	Coils	1.35	0.2	0.17	1.72
	Shield	12.1	24.2	9.5	45.7
CNAO	Coils	1.76	0.2	0.25	2.21
	Shield	37.9	24	12.55	74.4
CNAO Field ramp rate [T/s]		Q_{hyst} [W/m]	Q_{ifcc} [W/m]	Q_{iscc} [W/m]	Q_{tot} [W/m]
0.18		1.86	0.011	0.10	1.97

Acknowledgments
The authors would like to thank M. Pullia (CNAO) and S. Sanfilippo (PSI) for the valuable information on the resistive magnet design used for this analysis.

References
[1] Bisoffi G, Benedetto E, Karppinen M, Pullia M G, Khalvati M R, Rossi L, Sapinski M, Sorbi M, Valente U, van Weelderen R, Venchi G and Vretenar M 2023 *Journal of Physics: Conference Series* **2420**(1) 012109
[2] Mariotto S, Marinozzi V, Rysti J, Sorbi M and Statera M 2018 *IEEE Transactions on Applied Superconductivity* **28**(3) 1–5
[3] Mariotto S, Leone A, Paccalini A, Pasini A, Pedrini D, Quadrio M, Sorbi M, Statera M, Todero M and Valente R 2019 *IEEE Transactions on Applied Superconductivity* **29**(5) 1–5
[4] Mariotto S, Todero M, Valente R, Leone A, Paccalini A, Pasini A, Pedrini D, Prioli M, Quadrio M, Sorbi M and Statera M 2020 *IEEE Transactions on Applied Superconductivity* **30**(4) 1–5
[5] Mariotto S, Leone A, Matteis E D, Paccalini A, Palmisano A, Pasini A, Pedrini D, Prioli M, Sorbi M, Sorti S, Statera M, Todero M and Valente R U 2023 *IEEE Transactions on Applied Superconductivity* **33**(5) 1–5
[6] Konstantopoulou K, Ballarino A, Gharib A, Stimac A, Gonzalez M G, Fontenla A T P and Sugano M 2016 *Superconductor Science and Technology* **29**(8) 084005
[7] Matteis E D, Barna D, Ceruti G, Kirby G, Lecrevisse T, Mariotto S, Perini D, Prioli M, Rossi L, Scibor K, Statera M, Sorbi M, Sorti S, Toral F and Valente R 2023 *IEEE Transactions on Applied Superconductivity* 1–6
[8] Nakamoto T, Sugano M, Xu Q, Kawamata H, Enomoto S, Higashi N, Idesaki A, Iio M, Ikemoto Y, Iwasaki R, Kimura N, Ogitsu T, Okada N, ichi Sasaki K, Yoshida M and Todesco E 2015 *IEEE Transactions on Applied Superconductivity* **25**(3) 1–5
[9] Idesaki A, Nakamoto T, Yoshida M, Shimada A, Iio M, Sasaki K, Sugano M, Makida Y and Ogitsu T 2016 *Fusion Engineering and Design* **112** 418–424
[10] Alknes P, Hagner M, Bjoerstad R, Scheuerlein C, Bordini B, Sugano M, Hudspeth J and Ballarino A 2016 *IEEE Transactions on Applied Superconductivity* **26**(3)
[11] Alessandria F, Angius S, Bellomo G, Fabbricatore P, Farinon S, Gambardella U, Marabotto R, Musenich R, Repetto R, Sorbi M and Volpini G 2013 URL `https://www.openaccessrepository.it/record/21061`
[12] Sorbi M and Marinozzi V 2016 *IEEE Transactions on Applied Superconductivity* **26**(6)
[13] Wilson M N 1986 335
[14] Verweij A P 1995 URL `https://cds.cern.ch/record/292595`
[15] Fabbricatore P, Farinon S, Incardone S, Gambardella U, Saggese A and Volpini G 2009 *Journal of Applied Physics* **106**(8) 083905
[16] Cryomech - the original innovators URL `https://www.cryomech.com/`
[17] Prioli M, Matteis E D, Farinon S, Felcini E, Gagno A, Mariotto S, Musenich R, Pullia M, Rossi L, Sorbi M, Sorti S, Statera M and Valente R U 2023 *IEEE Transactions on Applied Superconductivity* **33**(5)